Reconfigurable Double-Stub Tuners Using MEMS Switches for Intelligent RF Front-Ends

John Papapolymerou, *Member, IEEE*, Krista L. Lange, Charles L. Goldsmith, *Senior Member, IEEE*, Andrew Malczewski, *Member, IEEE*, and Jennifer Kleber, *Member, IEEE*

***Abstract*—This paper presents novel planar dynamically reconfigurable double-stub tuners that utilize electrostatically activated microelectromechanical system (MEMS) switches. The tuners operate in the 10–20-GHz frequency range and have stubs that consist of a digital capacitor bank. Each bank has a predetermined number of capacitors that can be selected through the activation of appropriate MEMS switches. The value and number of capacitors is dictated by the range of loads that needs to be matched. Simulated and measured results from several designs are presented. A 4 bit $\times$ 4 bit tuner that can match loads with $1.5\ \Omega < \mathrm{Re}\{Z_L\} < 109\ \Omega$ and $-107\ \Omega < \mathrm{Im}\{Z_L\} < 48\ \Omega$ at 20 GHz equivalent to three quadrants of the Smith chart and loads with $3\ \Omega < \mathrm{Re}\{Z_L\} < 94\ \Omega$ and $-260\ \Omega < \mathrm{Im}\{Z_L\} < 91\ \Omega$ at 10 GHz is demonstrated for the first time, as well as other designs. The demonstrated tuners provide real-time reconfiguration and matching for RF loads that change values during system operation. Applications include the development of several novel highly integrated microwave/millimeter-wave circuits such as ultra-wide-band high output power and increased power-added-efficiency amplifiers, ultra-wide-band multipliers, and very broad-band antenna arrays. It is expected that these circuits will be part of future low-cost and low-power intelligent RF front-end microsystems and systems-on-a-chip.**

***Index Terms*—Intelligent RF front-ends, reconfigurable tuner, RF microelectromechanical system (MEMS) switches.**

I. Introduction

MICROWAVE and millimeter-wave technology that offers high-performance, low cost, small size, low power, and wide tunability is essential for today's cost-driven commercial and military industries. In order to meet the above requirements, the research community over the last ten years has been focusing on entire system-on-a-chip solutions, where different components (e.g., passive, active) are integrated on the same substrate. To enhance the performance of planar microwave circuits and address associated problems, researchers have been using micromachining techniques and microelectromechanical system (MEMS) devices [1].

Manuscript received October 29, 2001. This work was supported in part by the Raytheon Company under IDEA and IR&D funds and in part by the NSF-S/IUCRC Center for Low Power Electronics under Grant EEC-9523338.

J. Papapolymerou was with the Department of Electrical and Computer Engineering, The University of Arizona, Tucson, AZ 85721 USA. He is now with the School of Electrical and Computer Engineering, Georgia Institute of Technology, Atlanta, GA 30332 USA.

K. L. Lange is with the Raytheon Company, Tucson, AZ 85734 USA.

C. L. Goldsmith was with the Raytheon Company, Dallas, TX 75243 USA. He is now with the Memtronics Corporation, Plano, TX 75075 USA

A. Malczewski and J. Kleber are with the Raytheon Company, Dallas, TX 75243 USA.

Digital Object Identifier 10.1109/TMTT.2002.806513

One of the first MEMS devices developed for microwave applications was the switch. An air-bridge-type electrostatically activated switch that uses a very high capacitance variation and has very small loss, but a high actuation voltage, has been demonstrated [2], [3]. Switches with serpentine and cantilever springs that exhibit low pull-in voltages, small loss, and good isolation [4], as well as thermally actuated switches have also been demonstrated [5]. Micromachined varactors that exhibit a wide tuning range and are part of a low-noise voltage-controlled oscillator [6]–[8], as well as X- and K-band single-pole double-throw switching circuits [9] have also been demonstrated. A substantial amount of progress has also been reported in bulk micromachined passive and active microwave/millimeter-wave structures including planar transmission lines [10]–[12], filters [13], couplers [14], resonators [15], antennas [16], and other components.

This paper presents novel planar dynamically reconfigurable double-stub tuners that utilize electrostatically activated MEMS switches in a series configuration. Preliminary results have been reported in [17]. The goal is to achieve a planar tuner that can match a wide variety of loads (at least two quadrants of Smith-chart coverage) for frequencies ranging from 10 to 20 GHz. This component will be an essential part for intelligent RF front-ends of future systems such as highly tunable, low-cost, and low-power wireless and satellite communication networks and radars, tunable navigation and positioning systems, and seekers for smart weapons. Recently, reconfigurable low-pass and bandpass filters that will be part of such systems have been demonstrated with center frequencies ranging from 10 to 30 GHz [18], as well as impedance tuners with resonant unit cells and variable stub-lengths realized by micromachined capacitors and MEMS switches [19]. The latter tuner achieved a tuning range equivalent to two quadrants of the Smith chart and a maximum voltage standing-wave ratio (VSWR) of 32.3 at Ka-band. The tuner presented here achieves a higher tuning range and VSWR and uses a combination of MEMS switches and monolithic capacitors [20].

II. Reconfigurable Tuner Design

A double stub tuner, such as the one shown in Fig. 1(a), is a very commonly used impedance-matching network. In order to make this circuit reconfigurable and achieve a wide load matching capability, either the lengths of both stubs or the length of one stub and the distance between them needs to be changed significantly. Since changing the length between stubs is extremely difficult, for planar and highly integrated

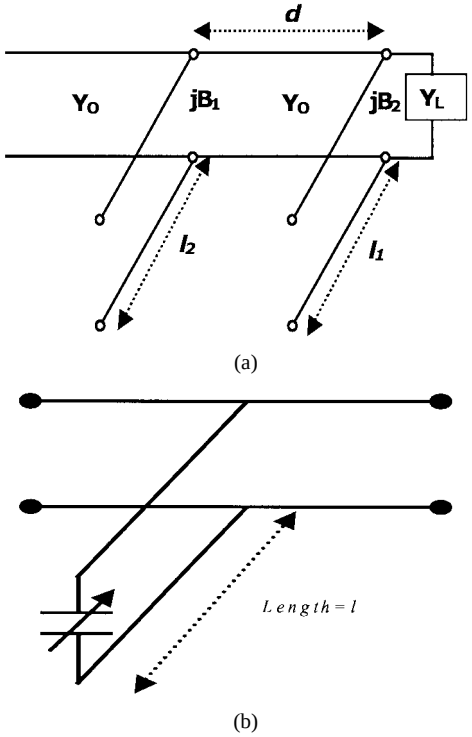

Fig. 1. (a) Schematic of double-stub tuner circuit. (b) Illustration of method of reconfiguring stub length with variable capacitance.

microwave/millimeter-wave circuits, reconfigurability can be achieved by fixing the various stub lengths and terminating each stub with a variable capacitance [see Fig. 1(b)]. Each time the capacitance at the end of the stub changes, the susceptance at the stub input changes allowing for a different load match. Given a range of loads that is desired to be matched, the stub susceptances (B_1 and B_2) and inter-stub distance [see Fig. 1(d)] can be determined analytically based on the procedure described in [21]. The smaller the range, the easier the circuit will be to realize, as will be shown with the different designs presented here. In order to investigate the potential of this technology, circuits that matched loads with $20\ \Omega < \mathrm{Re}\{Z_L\} < 80\ \Omega$ and $-150\ \Omega < \mathrm{Im}\{Z_L\} < 150\ \Omega$ to 50 Ω were designed first (the design procedure is similar for matching to a Z_0 other than 50 Ω).

Having chosen the necessary design parameters for the double-stub tuner circuit, a mathematical analysis can be performed to calculate the performance of the circuit. Given the stub spacing d, the range of G_L (the real part of the load admittance) that can be matched is given by [21] as

$$0 \le G_L \le \frac{Y_o}{\sin^2 \beta d} \tag{1}$$

where β is the phase constant of the transmission line connecting the two stubs.

One of the disadvantages of the double-stub tuner is that it cannot match all load impedances [20]. The design parameter that determines how large the "unmatchable" range will be is d, the distance between the stubs. The first step in the tuner design is to choose the distance d. The "unmatchable" range can be minimized by making d very small or very close to a multiple of $\lambda/2$. However, as d approaches zero (or $\lambda/2$), the circuit becomes more frequency sensitive. For this project, the distance d was chosen to be relatively small (0.1λ) to maximize the range of matchable loads while sacrificing the frequency sensitivity of the circuit. In a different design, a compromise between the frequency sensitivity and the "unmatchable" region could be chosen. If d is chosen to be 0.1λ, then $0 \le G_L \le 0.058$ or the real part of the load impedance ($R_L = 1/G_L$) must be greater than 17.3 Ω to be able to be matched to 50 Ω. In this case, since the real part of the load to be matched is 20-80 Ω, a distance of 0.1λ is sufficient. If a value of $R_L < 17.3\ \Omega$ was desired, d would need to be made smaller.

TABLE I
CALCULATED NECESSARY SUSCEPTANCE AND CAPACITANCE VALUES FOR THE STUBS TO MATCH THE DESIRED RANGE OF LOAD IMPEDANCES TO $Z_o = 50\ \Omega$ WITH A STUB SPACING OF $d = 0.1\lambda$

Load Impedance (Ohms)	B_1 (Ω^{-1})	Capacitance of Stub 1 (fF) 10 GHz	15 GHz	20 GHz	B2 (Ω^{-1})	Capacitance of Stub 2 (fF) 10 GHz	15 GHz	20 GHz
20 + j0	.047	754	503	377	.035	565	376	282
80 + j0	.051	817	545	409	.066	105	696	522
20 - j150	.028	446	297	223	.189	3010	2007	1505
20 + j150	.041	655	436	327	.189	3010	2007	1505
80 - j150	.035	552	368	276	.117	1859	1239	929
80 + j150	.045	717	478	359	.117	1859	1239	929

Once the distance between the stubs was chosen, the susceptances of each stub that would match the range of loads to 50 Ω were determined. The equations for the susceptances of the two stubs are [20]

$$B_1 = -B_L \pm \frac{Y_0 + \sqrt{(1+t^2)G_L Y_0 - G_L^2 t^2}}{t} \tag{2}$$

and

$$B_2 = \frac{\pm Y_0 \sqrt{(1+t^2)G_L Y_0 - G_L^2 t^2} + G_L Y_0}{G_L t} \tag{3}$$

where G_L and B_L are the real and imaginary parts of the load admittance, respectively, and $t = \tan \beta d$. The capacitance values associated with B can be calculated from

$$C = \frac{B}{2\pi f_d} \tag{4}$$

where f_d is the design frequency. Equations (2)–(4) were used to calculate the stub capacitances needed to match certain load impedances. The load impedances were chosen at the extremes of the design range. Table I displays the results of these calculations at three design frequencies (10, 15, and 20 GHz) assuming a characteristic impedance of $Z_o = 50\ \Omega$ and a stub spacing of $d = 0.1\lambda$.

The next step in the design is the implementation of the variable-susceptance stubs. Knowing that RF MEMS switches would be used to make the circuit reconfigurable, only the basic configuration of realizing the required fixed capacitance values had to be determined. In other words, knowing that the switches could be used in either the "on" or "off" positions, a way of switching through the range of desired capacitances (stub susceptances) was designed. Also considered was the number of capacitance values to be accessible between the minimum and maximum values. These considerations led to the

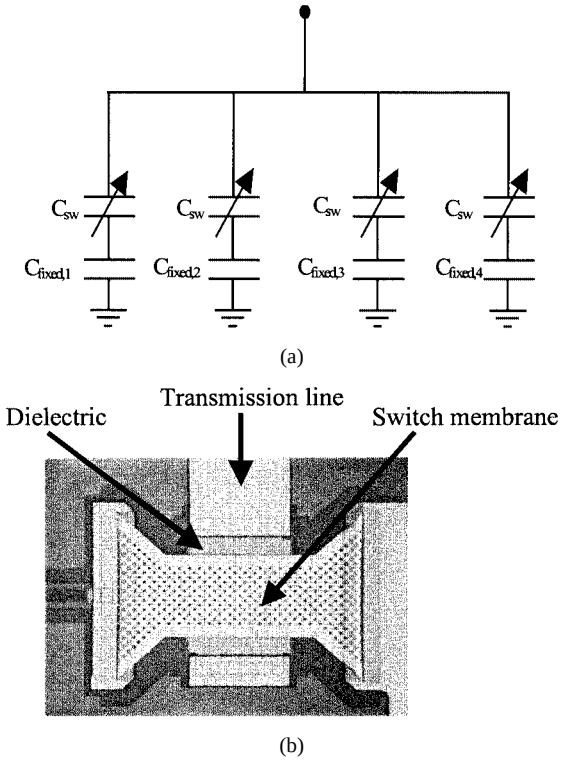

Fig. 2. (a) Schematic of a 4-bit reconfigurable stub that consists of fixed capacitors and MEMS switches. (b) Close-up photograph of capacitive "bow-tie" switch used in the tuner designs (dimensions are 280-μm long and 180-μm wide and the transmission line is 130-μm wide).

design concept shown in Fig. 2(a). The circuit consists of four sets of capacitors in parallel, but designs with two and three were also considered. The more sets used, the wider the range of load impedances that can be matched. If fewer sets are used, the more simplistic the circuit is to design and use. Also, the number of sets used will be determined by the amount of space available. Each set consists of the series combination of an RF MEMS switch and a fixed capacitor. The RF MEMS switch to be used [see Fig. 2(b)] has been studied before and its response has been well characterized [22]. In effect, the MEMS switch toggles the fixed capacitor "on" or "off." When the MEMS switch is in the "up" or "off" position, it has a capacitance value of approximately 35 fF. When it is in the "down" or "on" position, it has a capacitance value of approximately 3 pF [2]. The equivalent capacitance of the series combination of the MEMS switch and the fixed capacitor is then

$$C_{\text{eq}} = \frac{C_f \cdot C_s}{C_f + C_s} \tag{5}$$

where C_f is the value of the fixed capacitor and C_s is the capacitance of the MEMS switch. Thus, when the switch is in the "off" position, $C_s \ll C_f$ and $C_{\text{eq}} \sim C_s$. When the switch is in the "on" position, $C_f \ll C_s$ and, thus, $C_{\text{eq}} \sim C_f$.

The desired range of capacitances is achieved by using several sets of these series combinations of switches and fixed capacitors in parallel or a "digital" bank of capacitors. Each pair of switch and fixed capacitor represents 1 bit of equivalent capacitance. The more bits used, the larger the number of capacitance steps available and, thus, the larger the range of loads that can be matched. Designs with 2- and 4-bit stubs at $f_d = 20$ GHz and 2- and 3-bit stubs at $f_d = 10$ GHz were pursued. Using the results listed in Table I and choosing $f_d = 20$, it can be shown that to match the desired load impedance range, Stub 1 will need a capacitance range of 223–409 fF and Stub 2 will need a capacitance range of 282–1505 fF. These capacitance values represent the *equivalent* capacitance values consisting of all the switches and fixed capacitances together. A spreadsheet analysis was performed to determine what combination of fixed capacitance values was needed for each stub to cover the necessary equivalent-capacitance range. Also, the fixed capacitances were chosen such that a 1-bit change would always result in a fixed step value. In other words, as the bits are stepped through, one bit at a time, each change will produce the same delta capacitance value. For instance, for Stub 1, a step size of 25 fF was chosen. Since there are $2^4 = 16$ combinations for each stub, this gives a total range of 16×25 fF $= 400$ fF, more than enough to cover the $409 - 223 = 186$ fF range needed. Likewise, for Stub 2, a step size of 100 fF was chosen, resulting in a range of 16×100 fF $= 1600$ fF, which covers the needed range of $1505 - 282 = 1223$ fF. The required fixed capacitance values were calculated with an iterative method of assuming a value and observing how this affected the overall equivalent capacitance. Results can be seen in Table II. A similar analysis can be performed for the other stub designs.

TABLE II
CALCULATED FIXED CAPACITOR VALUES FOR 4-BIT STUBS WITH $f_d = 20$ GHz

Stub 1	Stub 2
45 fF	133 fF
76 fF	250 fF
133 fF	506 fF
250 fF	1155 fF

Since the operating frequency of the tuners was greater than 10 GHz, the fixed capacitors were realized with open-circuited microstrip stubs. The lines connecting the switch-stub sets were $0.5\lambda g$ long, or a multiple thereof, so that the capacitance values seen at the input of each set would be the same at the point where all sets meet. Likewise, the line connecting the point where all switch-stub sets meet to the main transmission line was also a multiple of $0.5\lambda g$. In order to predict as accurately as possible the performance of the double-stub tuners, the switch-stub sets combinations were simulated with Ansoft's HFSS that uses the finite-element method (FEM). Results from these simulations were incorporated into Agilent's HP-ADS that was used to simulate the entire tuner design. The simulated results are presented in the following sections. In terms of the tuner bandwidth, due to the nature of the connecting lines ($\lambda g/2$), a 10%–15% value is estimated. Table III summarizes the simulated results for the tuner bandwidth versus distance d for a given load. As seen in Table III, the simulations agree well with the expected results.

III. CIRCUIT FABRICATION

Several steps were involved in the fabrication of the reconfigurable double-stub tuner. Due to wafer space limitations, all

TABLE III
CALCULATED TUNER BANDWIDTH FOR VARIOUS INTER-STUB DISTANCES d FOR A SERIES RESISTOR AND INDUCTOR LOAD ($R = 82\ \Omega$, $L = 0.32$ nH). THE TUNER BANDWIDTH IS DEFINED BY THOSE FREQUENCIES WHERE THE MATCHED RETURN LOSS IS GREATER THAN 10 dB

Distance, d	0.1λg	0.2λg	0.3λg	0.4λg	0.5λg
Tuner BW	16.5%	15%	13%	10%	11.5%

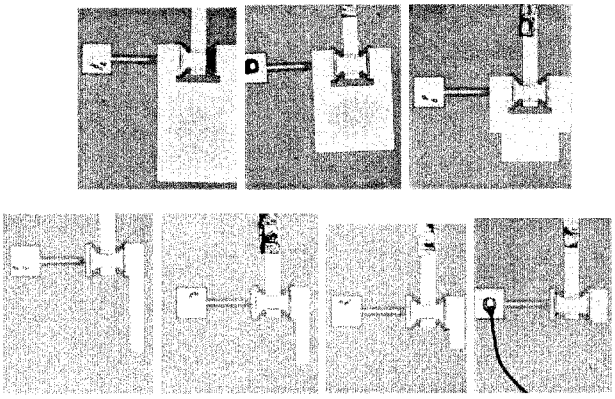

(a)

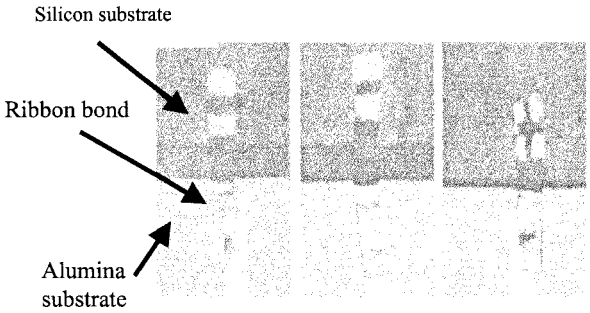

(b)

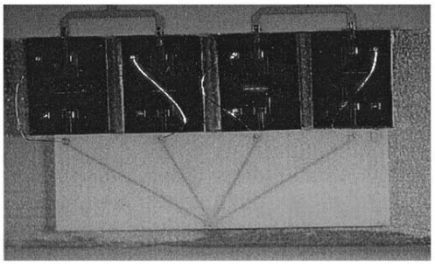

(c)

Fig. 3. (a) Fabricated switch-stub sets on silicon (Table II lists the desired capacitance values of the open-circuited stubs). (b) Photographs of ribbon bonds (5-mil wide) connecting the silicon substrates containing the switches to the alumina substrate. (c) Photograph illustrating wire bonds placed to connect the dc probe pads to the switches.

parts of the tuners could not be fabricated together. The capacitive membrane switches [see Fig. 2(b)] along with the open-circuited stubs were fabricated on a 500-μm-thick silicon substrate with a resistivity of 10 KΩ-cm. Details of the switch fabrication can be found in [22]. Some of the fabricated switch-stub combinations can be seen in Fig. 3(a). The remainder of the circuit, including the dc-bias lines, was fabricated on a 10-mil-thick alumina substrate with conventional lithographic techniques. The various silicon and alumina pieces were then assembled on a brass carrier using conductive epoxy. The switch-stub sets were connected to the alumina microstrip lines with 5-mil-wide gold ribbon bonds [see Fig. 3(b)], while the dc probe pads were connected with 1-mil-wide gold wire bonds [see Fig. 3(c)]. Ribbon bonds were chosen for the RF/microwave connection to minimize the parasitic inductance seen by the circuit. Pictures of the four assembled tuners can be seen in Fig. 4. Coplanar waveguide (CPW)-to-microstrip transitions were also included in the circuits to facilitate the measurements. The size of the 4 bit $\times$ 4 bit tuner excluding the transitions was approximately 18 mm $\times$ 11 mm.

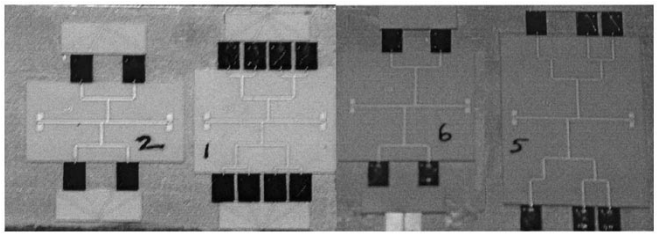

Fig. 4. Four fabricated tuners. From left to right: 20 GHz 2 bit $\times$ 2 bit, 20 GHz 4 bit $\times$ 4 bit, 10 GHz 2 bit $\times$ 2 bit, 10 GHz 3 bit $\times$ 3 bit.

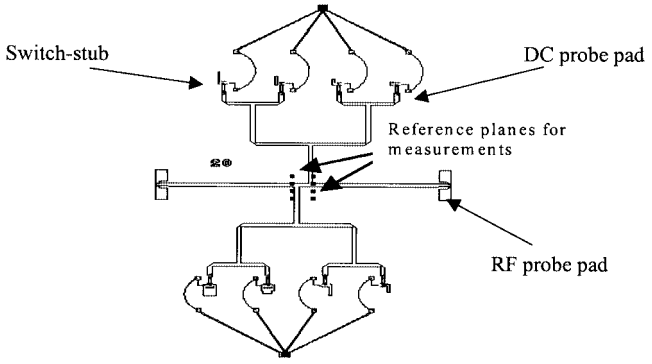

Fig. 5. Schematic of one tuner circuit showing the measurement reference planes.

IV. RESULTS

Measurements of the various circuits were taken with a vector network analyzer and an RF probe station using a thru-reflect line (TRL) calibration technique. The reference planes for the measurements were at the intersection points of the two stubs with the input/output microstrip line (see Fig. 5). GGB Industries RF probes with 150-μm pitch were used to probe the tuners, while Cascade Microtech probes with 150-μm pitch were used as the dc probes. Wires were soldered to the dc probe cards to provide a connection point for the switch actuation control signal. The dc voltage was applied to the membranes through the dc probe cards. Measurements were taken from 10 to 20 GHz and, for the "on" state of the MEMS switches, a dc voltage of 35–55 V was applied. At each data point (a unique combination of switch states), two-port S-parameter measurements were taken using the network analyzer. By mathematically applying a load on one port (in this case, 50 Ω), the input impedance can be

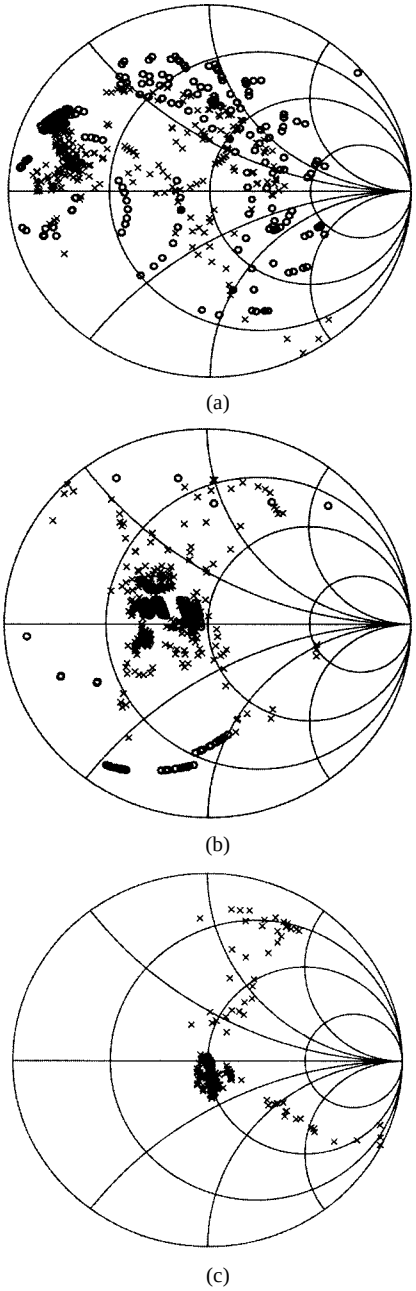

Fig. 6. Simulated (O) and measured (X) range of matched load impedances for the 20-GHz optimized 4 bit × 4 bit tuner at: (a) 20 GHz, (b) 15 GHz, and (c) 10 GHz.

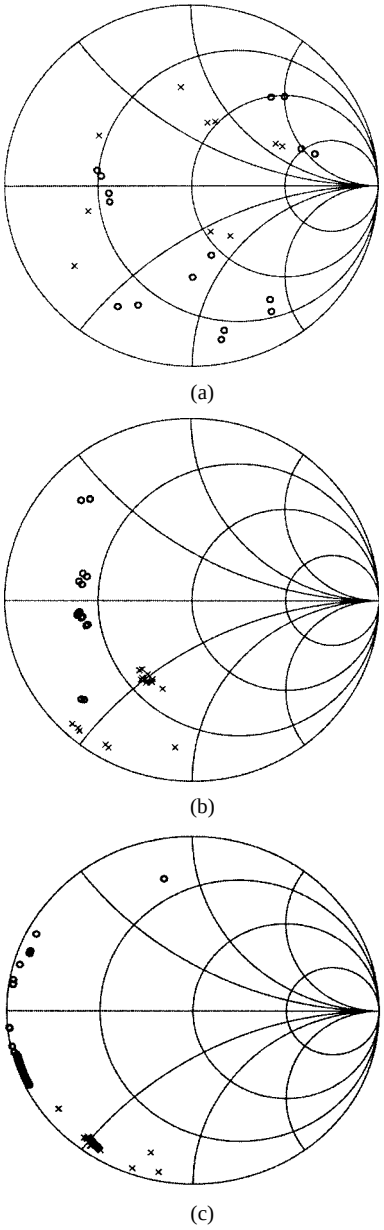

Fig. 7. Simulated (O) and measured (X) range of matched load impedances for the 20-GHz optimized 2 bit × 2 bit tuner at: (a) 20 GHz, (b) 15 GHz, and (c) 10 GHz.

calculated at the opposite port. The conjugate of this impedance is the value of the load impedance that can be matched with the circuit to 50 Ω. Measured and simulated results for all fabricated circuits are shown in Figs. 6–9.

Fig. 6 shows the results for the 20-GHz optimized 4 bit × 4 bit tuner circuit. As can be seen in Fig. 5(a), the tuner can match at 20-GHz load impedances with $1.5\ \Omega < \mathrm{Re}\{Z_L\} < 109\ \Omega$ and $-107\ \Omega < \mathrm{Im}\{Z_L\} < 48\ \Omega$. In addition, the measured and simulated results agree very well. This circuit by far provides the largest range of matchable load impedances equivalent to three quadrants of the Smith chart. This is due to the large number of bits used for each stub (in this case, four). It should be noted here that, out of the 256 possible loads that can be matched (256 different switch states), only 142 were measured. This was due to stiction problems caused by operating the switches in an open-air environment. The range, therefore, of matchable loads for this tuner is higher than the actual measured one (especially regarding the imaginary part of the load). This tuner can potentially cover all four quadrants of the Smith chart. Furthermore, measurements show that a maximum VSWR of 99 was achieved at the fourth quadrant and 15.7 at the second and third quadrants of the Smith chart. This is attributed to the low-loss nature of the MEMS components. Thus, the MEMS tuner performance is superior compared to conventional tuners using FET devices. At the other frequencies of 10 and 15 GHz, the range changes due to the changing values of the fixed capacitors at these frequencies. The range of load impedances that can be matched with this circuit at 10 GHz is $3\ \Omega < \mathrm{Re}\{Z_L\} < 94\ \Omega$ and $-260\ \Omega < \mathrm{Im}\{Z_L\} < 91\ \Omega$, and is equivalent to two quadrants of the Smith chart. At 15 GHz, this circuit can match load

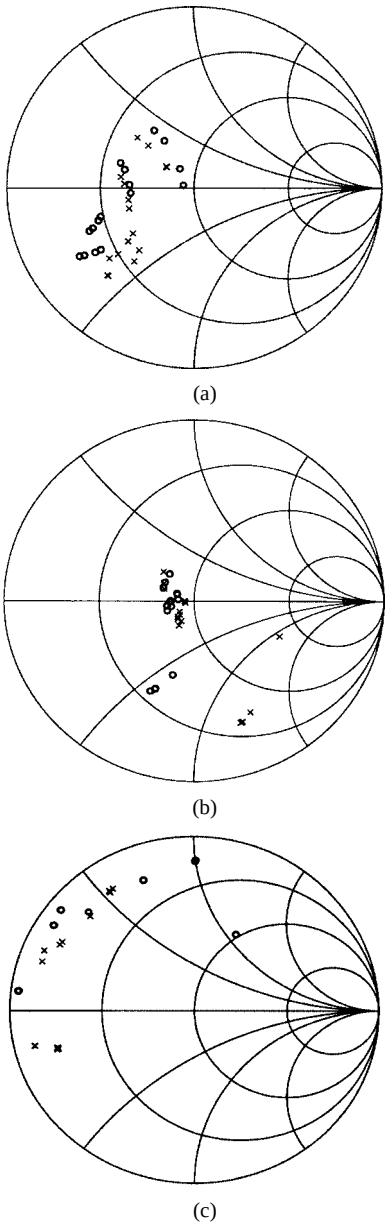

Fig. 8. Simulated (O) and measured (X) range of matched load impedances for the 10-GHz optimized 2 bit $\times$ 2 bit tuner at: (a) 10 GHz, (b) 15 GHz, and (c) 20 GHz.

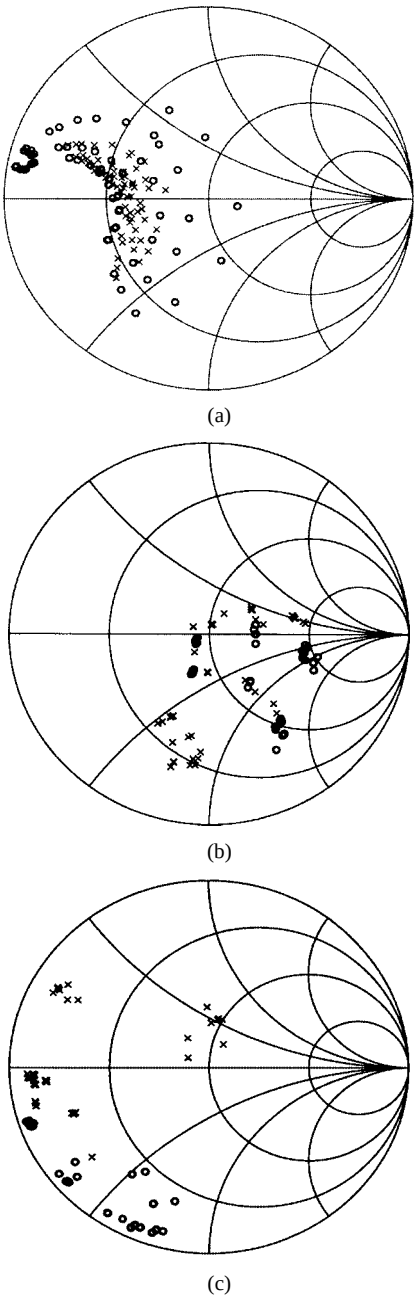

Fig. 9. Simulated (O) and measured (X) range of matched load impedances for the 10-GHz optimized 3 bit $\times$ 3 bit tuner at: (a) 10 GHz, (b) 15 GHz, and (c) 20 GHz.

impedances with $1\ \Omega < \mathrm{Re}\{Z_L\} < 155\ \Omega$ and $-68\ \Omega < \mathrm{Im}\{Z_L\} < 79\ \Omega$, equivalent to three quadrants of the Smith chart. Fig. 7 shows the results for the 20-GHz optimized 2 bit $\times$ 2 bit tuner circuit. Measurements indicate that, at 20 GHz, this tuner can match loads with $7\ \Omega < \mathrm{Re}\{Z_L\} < 115\ \Omega$ and $-40\ \Omega < \mathrm{Im}\{Z_L\} < -17\ \Omega$. Again, it is seen that the measured results agree well with the simulated results. While this tuner still covers a large range, similar to that described in the previous paragraph, because it only has 2 bits of capacitance per stub, the steps between the matched load impedances are much larger. This circuit also performed well at 10 and 15 GHz. At 10 GHz, the circuit can match load impedances with $1.3\ \Omega < \mathrm{Re}\{Z_L\} < 6.5\ \Omega$ and $-40\ \Omega < \mathrm{Im}\{Z_L\} < -17\ \Omega$, while at 15 GHz it can match loads with $1.8\ \Omega < \mathrm{Re}\{Z_L\} < 23\ \Omega$ and $-44\ \Omega < \mathrm{Im}\{Z_L\} < -22\ \Omega$.

Fig. 8 shows the results for the 10-GHz optimized 2 bit $\times$ 2 bit tuner. The measured results show that, at 10 GHz, this tuner can match load impedances in the range of $11\ \Omega < \mathrm{Re}\{Z_L\} < 36\ \Omega$ and $-21\ \Omega < \mathrm{Im}\{Z_L\} < 15\ \Omega$. Again, it is seen that the measured results agree well with the simulated results. While this circuit matches a smaller range of load impedances than the previous two circuits, the steps between the matched load impedances are much finer. This circuit exhibits similar performance at two other frequencies, i.e., 15 and 20 GHz. At 15 GHz, this circuit matches load impedances in the range of $23\ \Omega < \mathrm{Re}\{Z_L\} < 45\ \Omega$ and $-70\ \Omega < \mathrm{Im}\{Z_L\} < 12\ \Omega$. At 20 GHz, this circuit matches load impedances in the range

of $3\,\Omega < \mathrm{Re}\{Z_L\} < 7\,\Omega$ and $-7\,\Omega < \mathrm{Im}\{Z_L\} < 27\,\Omega$. Results for the 10-GHz optimized 3 bit $\times$ 3 bit tuner are shown in Fig. 9, where measurements indicate that, at 10 GHz, this tuner can match load impedances in the range of $7.8\,\Omega < \mathrm{Re}\{Z_L\} < 32.5\,\Omega$ and $-18\,\Omega < \mathrm{Im}\{Z_L\} < 12.5\,\Omega$. This circuit was also measured and simulated at 15 and 20 GHz. At 15 GHz, the circuit can match load impedances with $12\,\Omega < \mathrm{Re}\{Z_L\} < 140\,\Omega$ and $-68\,\Omega < \mathrm{Im}\{Z_L\} < 29\,\Omega$. At 20 GHz, the circuit can match load impedances in the range of $2\,\Omega < \mathrm{Re}\{Z_L\} < 56\,\Omega$ and $-8\,\Omega < \mathrm{Im}\{Z_L\} < 29\,\Omega$.

There are some minor discrepancies between the measured and simulated data that arise mostly from the variation of ribbon bond lengths and placements. In the HP-ADS simulations, each ribbon bond was assumed to be 300-μm long, which is an average of the various lengths of ribbon bonds placed by hand. Since the overall capacitance of each stub is determined by the addition of the capacitances of the switch-stub sets on each stub, the accuracy of this addition is dependent on the connecting microstrip lines being exactly half-wavelengths long. The latter makes the circuit extremely sensitive to variations in these half-wavelength lines. Since the ribbon bond is part of this half-wavelength line, its variation directly leads to variation in the performance of the circuit. In addition, the spacing between the alumina and the silicon substrates that were bonded together was not modeled in the HP-ADS simulations. Also, it should be noted that while the simulated and measured data agree fairly well at the design frequency, the two data sets agreed less at other frequencies. This again is due to the nature of the connecting lines being half-wavelengths long only at the optimized design frequency. At the other frequencies, these lines are closer to multiples of a quarter-wavelength. Thus, instead of transforming the switch-stub reactances a full rotation around the Smith chart, they are only transformed about halfway around the Smith chart. Any slight variations in circuit parameters (such as ribbon bond lengths and line lengths) have, therefore, a much larger effect on the circuit performance. These highly sensitive variations explain the discrepancies between the simulated and measured data at frequencies other than the optimized frequency for the circuit. It is believed that a complete monolithic fabrication of the tuner would minimize or eliminate these variations. The limitations of the current hybrid tuner approach are well understood and it is expected that a much better prediction of the matched loads and circuit reproducibility can be achieved with a completely monolithic approach. The monolithic approach will also lead to lower device cost. The hybrid tuner, however, allows for easy and fast fabrication and testing. Furthermore, the loss of the monolithic tuner will be similar to the hybrid one for a high-resistivity silicon wafer as the one used in this project.

Regarding the power-handling capability of the tuner, it is ultimately limited by the MEMS switches. These switches are designed to handle moderate power levels, approximately 1–2 W in a 50-Ω system. The switch voltage rating is limited by the pull-down voltage, while its current handling is limited by the maximum allowable current density in the switch metal layers. When the switches operate within resonant circuits, both voltage and current limits must be derated to account for the larger circulating voltages and currents that may be present.

V. Conclusions

Several planar reconfigurable double-stub tuners operating from 10–20 GHz have been designed, fabricated, and tested. Reconfigurability is achieved by selecting different open-circuited stubs via electrostatically activated MEMS switches. A 4 bit $\times$ 4 bit tuner was able to match loads with $1.5\,\Omega < \mathrm{Re}\{Z_L\} < 109\,\Omega$ and $-107\,\Omega < \mathrm{Im}\{Z_L\} < 48\,\Omega$ at 20 GHz covering three quadrants of the Smith chart and loads with $3\,\Omega < \mathrm{Re}\{Z_L\} < 94\,\Omega$ and $-260\,\Omega < \mathrm{Im}\{Z_L\} < 91\,\Omega$ at 10 GHz. A maximum VSWR of 99 and 15.7 was achieved at the fourth and second/third quadrants of the Smith chart, respectively. To the authors' knowledge, this is the largest matchable Smith-chart region reported thus far. 2 bit $\times$ 2 bit and 3 bit $\times$ 3 bit tuner designs were also demonstrated and achieved good performance. In addition, simulated results using Agilent's HP-ADS in combination with Ansoft's HFSS agreed well with measurements. Some discrepancies arose from the hybrid nature of the fabrication that included ribbon bonds connecting the silicon parts with the alumina parts of the circuit. Future development of these tuners in a totally monolithic fashion (estimated size $\sim$5–10 mm^2) will minimize these discrepancies, facilitate fabrication, lower cost, and improve performance and reproducibility. It is expected that the tuners that have been presented here will lead to more mature designs that will be part of an intelligent RF/microwave system-on-a-chip or system-on-a-package.

Acknowledgment

The authors would like to thank B. Rein, Raytheon Company, Tucson, AZ, for assisting with the wafer fabrication, as well as B. Pillans, Raytheon Company, Dallas, TX, and M. Eberly, Raytheon Company, Dallas, TX, for assisting with the tuner measurements and E. Zheng, Georgia Institute of Technology, Atlanta, for assisting with the tuner simulations.

References

[1] L. E. Larson, "Microwave MEMS technology for next-generation wireless communications," in *IEEE MTT-S Int. Microwave Symp. Dig.*, Anaheim, CA, June 1999, pp. 1073–1076.

[2] C. Goldsmith, S. Eshelman, and D. Denniston, "Performance of low-loss RF MEMS capacitive switches," *IEEE Microwave Guided Wave Lett.*, vol. 8, pp. 269–271, Aug. 1998.

[3] N. S. Barker and G. M. Rebeiz, "Distributed MEMS true-time delay phase shifters and wide-band switches," *IEEE Trans. Microwave Theory Tech.*, vol. 46, pp. 1881–1890, Nov. 1998.

[4] S. Pacheco, C. T. Nguyen, and L. P. B. Katehi, "Micromechanical electrostatic K-band switches," in *IEEE MTT-S Int. Microwave Symp. Dig.*, Baltimore, MD, June 1998, pp. 1569–1572.

[5] Z. Feng, W. Zhang, B. Su, K. Harsh, K. C. Gupta, V. Bright, and Y. C. Lee, "Design and modeling of RF MEMS tunable capacitors using electro-thermal actuators," in *IEEE MTT-S Int. Microwave Symp. Dig.*, Anaheim, CA, June 1999, pp. 1507–1510.

[6] ——, "Design and modeling of RF MEMS tunable capacitors using electro-thermal actuators," in *IEEE MTT-S Int. Microwave Symp. Dig. Digest*, Anaheim, CA, June 1999, pp. 1507–1510.

[7] D. J. Young and B. E. Boser, "A micromachined-based RF low-noise voltage-controlled oscillator," in *IEEE CICC Symp. Dig.*, 1997, pp. 431–434.

[8] H. D. Wu, K. F. Harsh, R. S. Irwin, A. R. Mickelson, Y. C. Lee, and J. B. Dobsa, "MEMS designed for tunable capacitors," in *IEEE MTT-S Int. Microwave Symp. Dig.*, 1998, pp. 127–129.

[9] S. Pacheco, D. Peroulis, and L. Katehi, "MEMS single-pole double throw (SPDT) X and K-band switching circuits," in *IEEE MTT-S Int. Microwave Symp. Dig.*, Phoenix, AZ, May 2001, pp. 321–324.

[10] L. P. B. Katehi, G. M. Rebeiz, and C. T.-C. Nguyen, "MEMS and micromachined components for low-power, high-frequency communication systems," in *IEEE MTT-S Int. Microwave Symp. Dig.*, Baltimore, MD, June 1998, pp. 331–333.
[11] L. P. B. Katehi and G. M. Rebeiz, "Novel micromachined approaches to MMIC's using low-parasitic, high-performance transmission media and environments," in *IEEE MTT-S Int. Microwave Symp. Dig.*, 1996, pp. 1145–1148.
[12] T. M. Weller, L. P. B. Katehi, and M. I. Herman, "New results using membrane-supported circuits: A Ka-band power amplifier and survivability testing," *IEEE Trans. Microwave Theory Tech.*, vol. 44, pp. 1603–1606, Sept. 1996.
[13] S. V. Robertson, L. P. B. Katehi, and G. M. Rebeiz, "Micromachined W-band filters," *IEEE Trans. Microwave Theory Tech.*, vol. 44, pp. 598–606, Apr. 1996.
[14] S. V. Robertson, A. R. Brown, L. P. B. Katehi, and G. M. Rebeiz, "A 10–60 GHz micromachined directional coupler," *IEEE Trans. Microwave Theory Tech.*, vol. 46, pp. 1845–1849, Nov. 1998.
[15] J. Papapolymerou, J. C. Cheng, J. East, and L. P. B. Katehi, "A micromachined high-Q X-band resonator," *IEEE Microwave Guided Wave Lett.*, vol. 7, pp. 168–170, June 1997.
[16] I. Papapolymerou, R. F. Drayton, and L. P. B. Katehi, "Micromachined patch antennas," *IEEE Trans. Antennas Propagat.*, vol. 46, pp. 275–283, Feb. 1998.
[17] K. Lange, J. Papapolymerou, C. Goldsmith, A. Malczewski, and J. Kleber, "A reconfigurable double stub tuner using MEMS devices," in *IEEE MTT-S Int. Microwave Symp. Dig.*, Phoenix, AZ, May 2001, pp. 337–340.
[18] D. Peroulis, S. Pacheco, K. Sarabandi, and L. Katehi, "Tunable lumped components with applications to reconfigurable MEMS filters," in *IEEE MTT-S Int. Microwave Symp. Dig.*, Phoenix, AZ, May 2001, pp. 341–344.
[19] H. T. Kim, S. Jung, K. Kang, J. H. Park, Y. Kim, and Y. Kwon, "Low-Loss analog and digital micromachined impedance tuners at the Ka-band," *IEEE Trans. Microwave Theory Tech.*, vol. 49, pp. 2394–2400, Dec. 2001.
[20] K. Lange, "A dynamically reconfigurable impedance tuner using RF MEMS switches," M.S. thesis, Dept. Elect. Comput. Eng., Univ. Arizona, Tucson, AZ, 2001.
[21] D. M. Pozar, *Microwave Engineering*. New York: Wiley, 1998.
[22] C. Goldsmith, A. Malczewski, Z. J. Yao, S. Chen, J. Ehmke, and D. H. Hinzel, "RF MEMS variable capacitors for tunable filters," *Int. J. RF Microwave Computer-Aided Eng.*, vol. 9, no. 4, pp. 362–374, July 1999.

John Papapolymerou (S'90–M'99) received the B.S.E.E. degree from the National Technical University of Athens, Athens, Greece, in 1993, and the M.S.E.E. and Ph.D. degrees from The University of Michigan at Ann Arbor, in 1994 and 1999, respectively.

From 1999 to 2001, he was a faculty member with the Department of Electrical and Computer Engineering, University of Arizona, Tucson. In August 2001, he joined the School of Electrical and Computer Engineering, Georgia Institute of Technology, Atlanta, where he is currently an Assistant Professor. His research interests include the implementation of micromachining techniques and MEMS devices in microwave, millimeter-wave, and terahertz circuits, and the development of both passive and active planar circuits on Si and GaAs for high-frequency applications.

Dr. Papapolymerou was the recipient of the 2002 National Science Foundation (NSF) CAREER Award and the 1997 Outstanding Graduate Student Instructional Assistant Award presented by the American Society for Engineering Education (ASEE), The University of Michigan Chapter. He was also the recipient of the 2002 Best Paper Award presented at the Third International Conference on Microwave and Millimeter-Wave Technology, China.

Krista L. Lange, photograph and biography not available at time of publication.

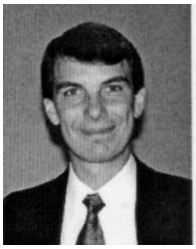

Charles L. Goldsmith (S'79–M'80–SM'94) received the B.S. and M.S. in electrical engineering from the University of Arizona, Tucson, in 1980 and 1982, respectively, and the Ph.D. degree from the University of Texas at Arlington, in 1995.

Since 1982, he has been involved in the design and development of microwave and millimeter-wave circuits and subsystems. He has been with M/A COM, Texas Instruments Incorporated, and most recently, was an Engineering Fellow with the Raytheon Company. Dr. Goldsmith recently formed his own company and is currently consulting and pursuing business opportunities in RF MEMS. Since 1993, he has developed RF MEMS devices and circuits and is the inventor of the capacitive membrane RF MEMS switch. He has spent the last several years dedicated to the development and application of these devices. These activities include the innovation of switches, phase shifters, and tunable antennas for radar and satcom applications, as well as variable capacitors and tunable filters for microwave receiver front-ends. He has authored or coauthored over 35 publications on microwave circuits, photonics, and RF MEMS. He recently completed the editing of a "Special Issue on RF Applications of MEMS Technology" for the *International Journal of RF and Microwave Computer-Aided Engineering* (New York: Wiley, 2001).

Dr. Goldsmith is a senior member of the IEEE Microwave Theory and Techniques Society (IEEE MTT-S) and the IEEE Laser and Electro-Optics Society (IEEE LEOS). He is a member of Tau Beta Pi. He has served as chairman and vice-chairman of the IEEE LEOS Dallas Chapter, currently serves on the IEEE MTT-12 Subcommittee on RF MEMS, and was recently a U.S. Delegate to the 7th World Micromachine Summit (2001), Freiburg, Germany.

Andrew Malczewski (S'93–M'96) was born in Warsaw, Poland, in May 1973. He received the Bachelor's degree in electrical engineering from the University of Texas at Arlington, in 1996, and is currently working toward the M.S. degree in electrical engineering at the University of Texas at Arlington.

Since 1996, he has been involved in the design and development of microwave and millimeter-wave circuits with the Raytheon Systems Company (formerly the Defense Electronics Group of Texas Instruments Incorporated), Dallas, TX. He is also involved in the development of RF MEMS technology for receiver and antenna applications.

Jennifer Kleber (S'92–M'00), photograph and biography not available at time of publication.